Archives of Hydro-Engineering and Environmental Mechanics
Vol. 52 (2005), No. 2, pp. 111–130

Calculating Effective Conductivity of Heterogeneous Soils by Homogenization

Adam Szymkiewicz

Institute of Hydro-Engineering of the Polish Academy of Sciences,
ul. Kościerska 7, 80-328 Gdańsk, Poland, e-mail: adams@ibwpan.gda.pl

(Received March 07, 2005; revised May 23, 2005)

Abstract

The paper concerns effective conductivity of a heterogeneous soil composed of two materials characterized by different hydraulic conductivities. According to the homogenization theory the effective conductivity is obtained from the solution of an elliptic equation for a single representative elementary volume. A numerical algorithm to solve this equation is described. Examples of calculations for periodic media with inclusions of various shapes are presented. Influence of volumetric fraction, arrangement, continuity and conductivity ratio of the two materials on the effective conductivity is investigated. Numerical results are compared with some analytical estimations available in the literature.

Key words: effective conductivity, soil heterogeneity, groundwater flow, up-scaling, homogenization

1. Introduction

Water flow in soils is commonly described by the following generalized equation, holding for both saturated and unsaturated conditions (e.g. Bear 1972, Zaradny 1993):

$$(C(h) + c_s S)\frac{\partial h}{\partial t} - \nabla \cdot (\mathbf{K}(h)\nabla(h + x_3)) = 0, \tag{1}$$

where $C(h)$ is the specific moisture capacity, c_s the specific storage coefficient, S saturation of the water phase, $\mathbf{K}(h)$ the hydraulic conductivity tensor, h the water pressure head (also known as suction head or capillary head in the unsaturated zone), x_3 the vertical coordinate. In the saturated zone $h > 0$, $C = 0$, $S = 1$ and $\mathbf{K}$ is independent of h. In unsaturated conditions $h < 0$, $S < 1$, the coefficients C and $\mathbf{K}$ are nonlinear functions of h, and the term $c_s S$ is negligibly small compared to C. Eq. (1) is valid on the assumption that the air phase filling pore space is at constant atmospheric pressure.

In practical applications one often has to deal with heterogeneous soils containing shales, lenses or other inclusions, characterized by the hydraulic conductivity $\mathbf{K}_2(h)$ very different from the conductivity of the base material (matrix) $\mathbf{K}_1(h)$, as shown in Fig. 1. If the modelled domain contains a large number of such inclusions, the local variability of $\mathbf{K}$ is difficult to account for in the solution of Eq. (1). In such case it is convenient to describe the flow at macroscopic scale, where the soil is considered to be homogeneous and characterized by effective (macroscopic) capacity $C^{eff}(h)$ and effective conductivity $\mathbf{K}^{eff}(h)$.

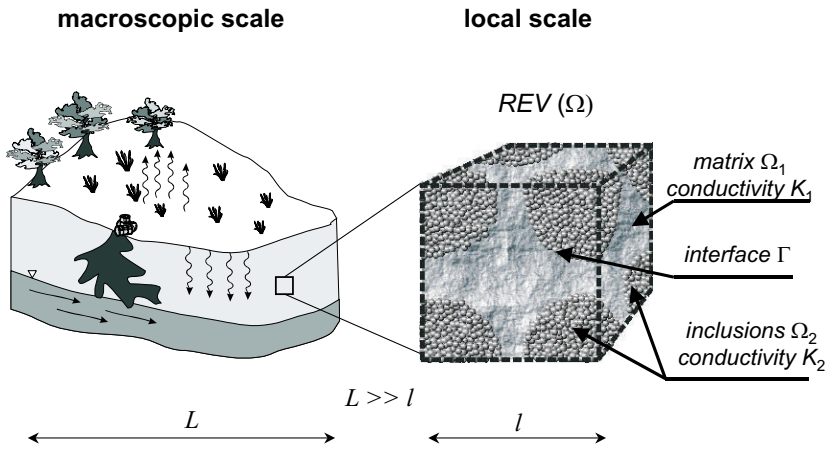

Fig. 1. Observation scales in a heterogeneous soil

The macroscopic equations can be derived from the local-scale equations using various mathematical techniques. One possible choice is the asymptotic homogenization method (Bensoussan et al. 1978, Sanchez-Palencia 1980, Auriault 1991). Application of this method to the problem of unsaturated flow in heterogeneous soils is described in the papers by Lewandowska & Laurent (2001), Lewandowska & Auriault (2004) and Lewandowska et al. (2004). These papers present macroscopic equations and definitions of the effective conductivity $\mathbf{K}^{eff}(h)$ and the effective capacity $C^{eff}(h)$ for three different cases: (1) moderately heterogeneous soil with local parameters of the same order, (2) soil with highly conductive inclusions and (3) soil with weakly conductive inclusions. In each model the effective conductivity coefficient is obtained from the solution of the local boundary value problem for an elliptic equation in the domain of a single representative elementary volume (REV). The models were validated by comparison with the results of "numerical experiments", i.e. direct solution of the local scale equation in heterogeneous domain (e.g. Lewandowska et al. 2004, Szymkiewicz 2004). Some preliminary results concerning comparison with laboratory experiments are also available (Lewandowska et al. 2005).

Apart from the derivation of a complete macroscopic description, a large amount of research has been focused solely on the estimation of the effective conductivity $\mathbf{K}^{eff}$ for heterogeneous media. From the point of view of the macroscopic description, such information is sufficient for steady flow. An overview of the methods employed to calculate the effective hydraulic conductivity (or permeability) is presented in the papers by Wen & Gomez-Hernandez (1996) and Renard & de Marsily (1997). The most popular approaches include direct numerical solution of the flow equation in a REV domain (Harter & Knudby 2004), renormalization (King 1989) and self-consistent methods (Dagan 1989, Poley 1988). One should note that the problem of calculating the effective transport properties concerns all physical processes described by equations similar to Eq. (1), e.g. thermal or electric conduction, diffusion, etc. – see for example, the works of Markov (1999) or Berryman (1995).

This paper aims to present the numerical calculation of the effective conductivity according to the asymptotic homogenization theory. The numerical results obtained for model soils of periodic structure with two- or three- dimensional inclusions will be compared with some analytical estimations available in the literature.

The following notation will be used throughout the paper. The conductivities of the two components are denoted by $\mathbf{K}_1$ and $\mathbf{K}_2$ (tensors) if the materials are anisotropic or K_1 and K_2 (scalars) if they are isotropic. The effective conductivity tensor is denoted by $\mathbf{K}^{eff}$ and its elements by K_{ij}^{eff}. If the effective conductivity is isotropic it is denoted as scalar K^{eff}.

2. Analytical Estimations of the Effective Conductivity

Consider a heterogeneous soil composed of two isotropic materials with the conductivity of K_1 and K_2, and volumetric fractions f_1 and f_2, respectively. For any spatial arrangement of the materials the elements of the effective conductivity tensor are bound in the following manner (e.g. Markov 1999):

$$\left(f_1 K_1^{-1} + f_2 K_2^{-1}\right)^{-1} = K^h \leq K_{ij}^{eff} \leq K^a = f_1 K_1 + f_2 K_2. \tag{2}$$

The bounds (2) are known as Wiener or Voigt-Reuss bounds. The upper and lower bounds correspond respectively to the weighted arithmetic mean K^a and weighted harmonic mean K^h of the components' conductivities. These two means are the exact values of K_{ij}^{eff} in perfectly layered soil, respectively for flow in the direction parallel (K^a) or orthogonal (K^h) to the layers. Thus, a layered arrangement of components shows the largest anisotropy. In all other cases K_{ij}^{eff} is somewhere between the harmonic and arithmetic mean. Obviously, the larger the difference between the components' conductivities, the wider the range of the admissible values of the effective conductivity.

The effective conductivity of heterogeneous media is commonly estimated using the effective medium theory. It focuses on the analysis of the perturbation of the potential field (pressure field in this case) caused by the presence of a single inclusion of different conductivity in a homogeneous material. On this basis, the effective conductivity for a material containing random dispersion of inclusions is estimated. Different variants of the effective medium methods exist (e.g. self-consistent or differential approach). Their application is described, for example, in the contributions of Markov (1999), Dagan (1989), Giordano (2003), Jones & Friedman (2000) or Fokker (2001).

One of the well-known results concerns macroscopically isotropic medium with 3D spherical or 2D circular inclusions. The effective conductivity is given by the following formula (e.g. Markov 1999):

$$K^{eff} = K_1 \frac{K_2 + (D-1)\,K_1 - (D-1)\,f_2\,(K_2 - K_1)}{K_2 + (D-1)\,K_1 + f_2\,(K_2 - K_1)}, \tag{3}$$

where indices 1 and 2 denote matrix and inclusion parameters respectively and D is the number of dimensions ($D = 2$ or 3). Eq. (3) is known as Maxwell's formula for $D = 3$ or Raleigh's formula for $D = 2$ (different names are also used). Hashin & Shtrikman (1962) showed that, for a macroscopically isotropic medium composed of two materials of the conductivity K_1 and K_2, arbitrarily arranged in space, Eq. (3) provides the maximum value of K^{eff} when $K_1 > K_2$ and the minimum value of K^{eff} when $K_1 < K_2$. Thus, the values obtained from Eq. (3) are known as Hashin-Shtrikman bounds. The other bounding value for each case mentioned can be obtained by interchanging K_1 with K_2 and f_1 with f_2 in Eq. (3).

The effective medium theory has also been applied to anisotropic media. The effective conductivity coefficient for a medium containing a dispersion of uniformly aligned ellipsoids is given by the following formula (Berryman 1995, Giordano 2003):

$$K_{ii}^{eff} = K_1 + f_2\,(K_2 - K_1)\left[1 + f_1 p_i\,(K_2 - K_1)\,(K_1)^{-1}\right]^{-1}, \tag{4}$$

where p_i is the depolarising factor in the direction i, assuming values from the range $\langle 0; 1\rangle$, while $p_1 + p_2 + p_3 = 1$. Note that in this case the effective conductivity is a diagonal tensor, the main anisotropy axes being parallel to the ellipsoids' axes. The depolarising factors depend on the shape of the ellipsoid and are defined by the following elliptic integral:

$$p_i = \frac{a_1 a_2 a_3}{2} \int_0^{+\infty} \frac{\mathrm{d}u}{\left(u + a_i^2\right)\sqrt{\left(u + a_1^2\right)\left(u + a_2^2\right)\left(u + a_3^2\right)}} \quad i = 1, 2, 3, \tag{5}$$

where a_1, a_2 and a_3 denote the lengths of the ellipsoid axes parallel to the respective directions. The computation of the depolarising factors for various geometries is presented in detail by Markov (1999) and Giordano (2003). For ellipses they can be calculated from Eq. (5), assuming that $a_3 \to \infty$. In this case $p_1 + p_2 = 1$, while $p_3 = 0$. For inclusions in the form of a circle ($p_1 = p_2 = 1/2$) or sphere ($p_1 = p_2 = p_3 = 1/3$) Eq. (4) reduces to Eq. (3). For inclusions in the form of layers orthogonal to p_1 direction $p_1 = 1$, $p_2 = p_3 = 0$ and Eq. (4) gives the harmonic mean of K_1 and K_2. One should note, however, that for anisotropic ellipses and ellipsoids Eq. (4) does not define bounds of the effective conductivity, contrary to Eq. (3).

Both presented formulae have been derived for the assumption that the volumetric fraction of inclusions is small ($f_2 \ll 1$), and the interaction between inclusions can be neglected. For larger volumetric fraction of inclusions one can use Bruggemann's formula in the following form (Berryman 1995, Giordano 2003):

$$f_1 (K_2 - K_1) (K_1)^{-p_i} = \left(K_2 - K_{ii}^{eff}\right) \left(K_{ii}^{eff}\right)^{-p_i}. \tag{6}$$

In this case K_{ii}^{eff} is given implicitly and Eq. (6) has to be solved by a numerical method.

3. Definition of the Effective Conductivity According to the Homogenization Theory

Consider a soil composed of two materials (anisotropic in a general case) of the conductivities $\mathbf{K}_1$ and $\mathbf{K}_2$ and the volumetric fractions f_1 and f_2. The soil has periodic structure. The REV (representative elementary volume, equivalent to period) is denoted by Ω, its parts occupied by the two materials by Ω_1 and Ω_2, respectively, and the interface between them by Γ. The dimension of the REV is very small compared to the dimensions of the considered macroscopic domain (Fig. 1), i.e. the following relation holds:

$$\varepsilon = \frac{l}{L} \ll 1, \tag{7}$$

where ε is scale parameter, l is the REV dimension, L is the dimension of the macroscopic domain. Eq. (1) represents a necessary condition for the existence of a macroscopic model. According to the homogenization theory the effective conductivity of such medium is defined as (Lewandowska & Laurent 2001):

$$\mathbf{K}^{eff} = \frac{1}{|\Omega|} \left[\int_{\Omega_1} \left(\mathbf{K}_1 \nabla \left(\boldsymbol{\chi}^I + \mathbf{y} \right) \right) \mathrm{d}\Omega + \int_{\Omega_2} \left(\mathbf{K}_2 \nabla \left(\boldsymbol{\chi}^{II} + \mathbf{y} \right) \right) \mathrm{d}\Omega \right], \tag{8}$$

where $|\Omega|$ is the REV volume, $\mathbf{y} = [y_1, y_2, y_3]$ is the local spatial coordinate associated with the REV and the vector function $\boldsymbol{\chi} = [\chi_1, \chi_2, \chi_3]$ is the solution of the following equation:

$$\nabla \cdot \mathbf{K}_1 \nabla \left(\boldsymbol{\chi}^I + \mathbf{y} \right) = 0 \quad \text{in} \quad \Omega_1, \tag{9a}$$

$$\nabla \cdot \mathbf{K}_2 \nabla \left(\boldsymbol{\chi}^{II} + \mathbf{y} \right) = 0 \quad \text{in} \quad \Omega_2, \tag{9b}$$

with $\boldsymbol{\chi} = \boldsymbol{\chi}^I$ in Ω_1 and $\boldsymbol{\chi} = \boldsymbol{\chi}^{II}$ in Ω_2. At the interface Γ the function $\boldsymbol{\chi}$ and its "flux" $\mathbf{K}\nabla(\boldsymbol{\chi} + \mathbf{y})$ are continuous:

$$\boldsymbol{\chi}^I = \boldsymbol{\chi}^{II} \quad \text{on} \quad \Gamma, \tag{10}$$

$$\mathbf{K}_1 \nabla \left(\boldsymbol{\chi}^I + \mathbf{y} \right) \mathbf{N} = \mathbf{K}_2 \nabla \left(\boldsymbol{\chi}^{II} + \mathbf{y} \right) \mathbf{N} \quad \text{on} \quad \Gamma, \tag{11}$$

where $\mathbf{N}$ is a unit vector normal to Γ. The function $\boldsymbol{\chi}$ is $\mathbf{y}$-periodic:

$$\boldsymbol{\chi}(y_i) = \boldsymbol{\chi}(y_i + l_i), \tag{12}$$

where l_i is the REV dimension in the specific direction y_i. For such boundary problem an infinite number of solutions exists, which differ by a constant value. In order to obtain a unique solution we assume that the average of function $\boldsymbol{\chi}$ in Ω is equal to zero:

$$\frac{1}{|\Omega|} \int_{\Omega} \boldsymbol{\chi} \, \mathrm{d}\Omega = 0. \tag{13}$$

Equations (9a, b) with the conditions (10)–(13) are known as the local boundary value problem. Its solution can be considered as equivalent to the solution of steady flow equation in a single REV with unit pressure gradient in directions y_1, y_2 and y_3, respectively. In scalar notation one obtains three equations – one for each component of $\boldsymbol{\chi}$. If both materials are locally isotropic, the equations have the following form:

$$\frac{\partial}{\partial y_1}\left(K \frac{\partial \chi_1}{\partial y_1} + K \right) + \frac{\partial}{\partial y_2}\left(K \frac{\partial \chi_1}{\partial y_2} \right) + \frac{\partial}{\partial y_3}\left(K \frac{\partial \chi_1}{\partial y_3} \right) = 0, \tag{14}$$

$$\frac{\partial}{\partial y_1}\left(K \frac{\partial \chi_2}{\partial y_1} \right) + \frac{\partial}{\partial y_2}\left(K \frac{\partial \chi_2}{\partial y_2} + K \right) + \frac{\partial}{\partial y_3}\left(K \frac{\partial \chi_2}{\partial y_3} \right) = 0, \tag{15}$$

$$\frac{\partial}{\partial y_1}\left(K \frac{\partial \chi_3}{\partial y_1} \right) + \frac{\partial}{\partial y_2}\left(K \frac{\partial \chi_3}{\partial y_2} \right) + \frac{\partial}{\partial y_3}\left(K \frac{\partial \chi_3}{\partial y_3} + K \right) = 0, \tag{16}$$

where $K = K_1$, $\boldsymbol{\chi} = \boldsymbol{\chi}^I$ in Ω_1 and $K = K_2$, $\boldsymbol{\chi} = \boldsymbol{\chi}^{II}$ in Ω_2. In this case the elements of the conductivity tensor:

$$\mathbf{K}^{eff} = \begin{bmatrix} K_{11}^{eff} & K_{12}^{eff} & K_{13}^{eff} \\ K_{21}^{eff} & K_{22}^{eff} & K_{23}^{eff} \\ K_{31}^{eff} & K_{32}^{eff} & K_{33}^{eff} \end{bmatrix}, \tag{17}$$

are defined in the following manner:

$$K_{ij}^{eff} = \frac{1}{|\Omega|}\left[\int_{\Omega_1}\left(K_1\frac{\partial \chi_i}{\partial y_j} + K_1\right)\mathrm{d}\Omega + \int_{\Omega_2}\left(K_2\frac{\partial \chi_i}{\partial y_j} + K_2\right)\mathrm{d}\Omega\right] \quad i = j, \tag{18}$$

$$K_{ij}^{eff} = \frac{1}{|\Omega|}\left[\int_{\Omega_1}\left(K_1\frac{\partial \chi_i}{\partial y_j}\right)\mathrm{d}\Omega + \int_{\Omega_2}\left(K_2\frac{\partial \chi_i}{\partial y_j}\right)\mathrm{d}\Omega\right] \quad i \neq j. \tag{19}$$

The effective conductivity is a function of the conductivities of both materials and of the local geometry. The influence of the REV geometry is represented by the function $\boldsymbol{\chi}$. Note that for a perfectly layered soil analytical solution of the problem (9)–(13) is possible, yielding K_{ij}^{eff} equal to the arithmetic or harmonic mean of the components' conductivities, which coincides with Eq. (2).

The definition (8)–(13) was obtained under the assumption that the hydraulic conductivities of the two materials $\mathbf{K}_1$ and $\mathbf{K}_2$ are of the same order (Lewandowska & Laurent 2001). However, it can be shown that the definition has a more general character and is applicable regardless of the local conductivity ratio (Szymkiewicz 2004). It is valid for soils with inclusions, as well as for soils composed of two interconnected materials. Similar definitions of the effective conductivity were proposed by other authors for single-phase and two-phase flow, using asymptotic homogenization (e.g. Saez et al. 1989) or volume averaging (e.g. Quintard & Whitaker 1988).

For flow in partially saturated conditions $\mathbf{K}_1$ and $\mathbf{K}_2$ as well as $\mathbf{K}^{eff}$ are functions of the pressure head h. A single point of the $\mathbf{K}^{eff}(h_i)$ function is obtained assuming the same value of the pressure head h_i in Ω_1 and Ω_2, and solving the local boundary value problem (9)–(13) with $\mathbf{K}_1 = \mathbf{K}_1(h_i)$ and $\mathbf{K}_2 = \mathbf{K}_2(h_i)$. Repeating this procedure for several values of h_i one obtains the function $\mathbf{K}^{eff}(h)$ in tabularized form (Lewandowska & Laurent 2001).

4. Numerical Solution of the Local Boundary Value Problem

The results presented in this paper were obtained using a numerical code developed by the author, based on the finite volume method (FVM). FVM is relatively simple in implementation and well suited for elliptic equations with discontinuous coefficients (Crumpton et al. 1995).

The REV domain Ω is divided into $M = M_1 \times M_2 \times M_3$ uniform cuboids (finite volumes or cells) of the dimensions $\Delta y_1 \times \Delta y_2 \times \Delta y_3$ (Fig. 2). Each volume

is characterized by a scalar hydraulic conductivity K_1 or K_2. The values of $\boldsymbol{\chi}$ are sought for at the geometrical centres of the volumes. The solution procedure is outlined on the example of Eq. (14) defining the component χ_1.

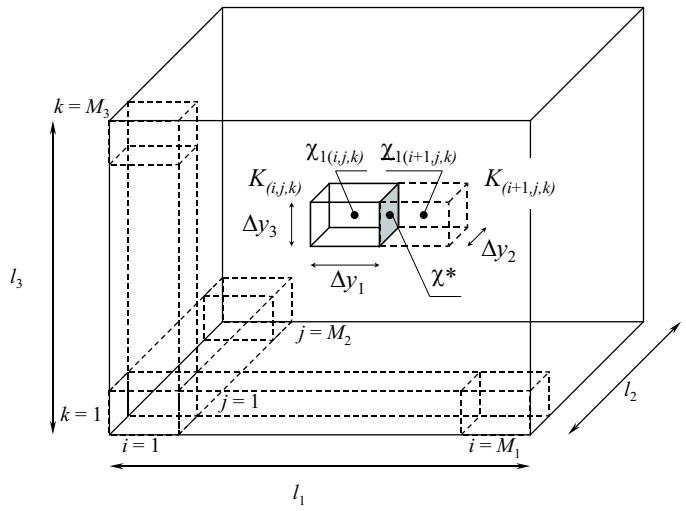

Fig. 2. Discretization of the REV domain for the solution of the local boundary value problem

According to the standard FVM procedure Eq. (14) can be written for each finite volume in the following conservative form:

$$\int_V (\nabla \cdot K \nabla (\chi_1 + y_1))\, \mathrm{d}V = \int_S (K \nabla (\chi_1 + y_1))\, \mathbf{n} \mathrm{d}S = \sum\nolimits_{l=1}^{6} q_l A_l, \qquad (20)$$

where K stands for either K_1 or K_2, V and S denote the volume and the external surface of the cell, $\mathbf{n}$ is a unit vector normal to S, q_l is the „flux" at each of the 6 sides of the cell, and A_l the side's surface. At the sides orthogonal to the y_1 axis q is equal to:

$$q = K \frac{\partial \chi_1}{\partial y_1} + K, \qquad (21)$$

while at the other sides:

$$q = K \frac{\partial \chi_1}{\partial y_i}, \qquad (22)$$

where $i = 2$ or 3. The fluxes q_l are approximated using the continuity conditions for the function χ_1 and its flux (10)–(11). For the flux q between the cells $(i,\ j,\ k)$ and $(i + 1, j, k)$ having (in a general case) different hydraulic conductivities $K_{(i,j,k)}$ and $K_{(i+1,j,k)}$ (Fig. 2) the continuity conditions yield:

$$K_{(i,j,k)}\frac{\chi^* - \chi_{1(i+1,j,k)}}{\frac{1}{2}\Delta y_1} + K_{(i,j,k)} = q = K_{(i+1,j,k)}\frac{\chi_{1(i+1,j,k)} - \chi^*}{\frac{1}{2}\Delta y_1} + K_{(i+1,j,k)}, \quad (23)$$

where χ^* is the value of χ_1 at the side's centre. The formula for q resulting from (23) is:

$$q = \frac{2K_{(i,j,k)}K_{(i+1,j,k)}}{K_{(i,j,k)} + K_{(i+1,j,k)}}\frac{\chi_{(i+1,j,k)} - \chi_{(i,j,k)}}{\Delta y_1} + \frac{2K_{(i,j,k)}K_{(i+1,j,k)}}{K_{(i,j,k)} + K_{(i+1,j,k)}}. \quad (24)$$

As can be seen, the hydraulic conductivity at the cell's side is equal to the harmonic mean of the neighbouring cells' conductivities. The fluxes at the other sides of the cell are approximated in the same manner. For the cells adjacent to the external boundary of the domain Ω one makes use of the periodicity conditions. Consider, for example, the approximation of fluxes in y_1 direction. The formula analogous to Eq. (24) written for the external sides of boundary cells $(1, j, k)$ and (M_1, j, k) would involve the values of $\chi_{1(0,j,k)}$ and $\chi_{1(M_1+1,j,k)}$ corresponding to the fictional cells adjacent to the boundary, but lying outside the solution domain. Due to periodicity conditions these values can be replaced by their counterparts from the opposite boundary: $\chi_{1(0,j,k)} = \chi_{1(M_1,j,k)}$ and $\chi_{1(M_1+1,j,k)} = \chi_{1(1,j,k)}$. Finally, in order to obtain a unique solution of Eq. (14) (and to satisfy Eq. (13)) the value $\chi_1 = 0$ should be specified at a single point of the solution domain.

Spatial discretization of Eq. (14) performed in the manner presented above leads to a system of linear algebraic equations with sparse and banded coefficient matrix (the maximum number of non-zero elements in a single row is 5 for a 2D problem and 7 for a 3D problem). The system is solved using the conjugated gradient method (Björck & Dahlquist 1974). Having obtained the values of $\chi_{1(i,j,k)}$ one can compute the integrals (18) and (19). The gradients of χ_1 appearing in the integrals are approximated numerically according to Eqs. (21)–(24).

5. Examples

5.1. Local Geometry and Numerical Parameters

The calculations were performed for soils of periodic structure. The representative elementary volume (period) is a rectangle of dimensions $l_1 \times l_2$ or a cuboid of dimensions $l_1 \times l_2 \times l_3$. The soil is composed of the base material (matrix) with the conductivity of K_1 and embedded inclusions with the conductivity of K_2 (both materials are locally isotropic). In three-dimensional case the inclusions have forms of cuboids, ellipsoids and octahedra (bipyramids) (Fig. 3). Their 2D analogues are rectangles, ellipses and rhombi. The inclusions are of uniform size and orientation, their dimensions in the directions y_1, y_2 and y_3 being denoted by a_1, a_2 and a_3. Two types of arrangements are studied (Fig. 3): simple arrangement (the centres

of inclusions are placed in the corners of the REV) and centred arrangement (the centres of inclusions are placed in the corners and in the centre of the REV). The inclusions are allowed to overlap. Note that all geometries are symmetric with respect to the coordinate axes (or planes). Thus, the effective conductivity tensor has off-diagonal elements equal to zero. The effective conductivity does not depend on the unit system, so in most of the examples dimensionless values will be used.

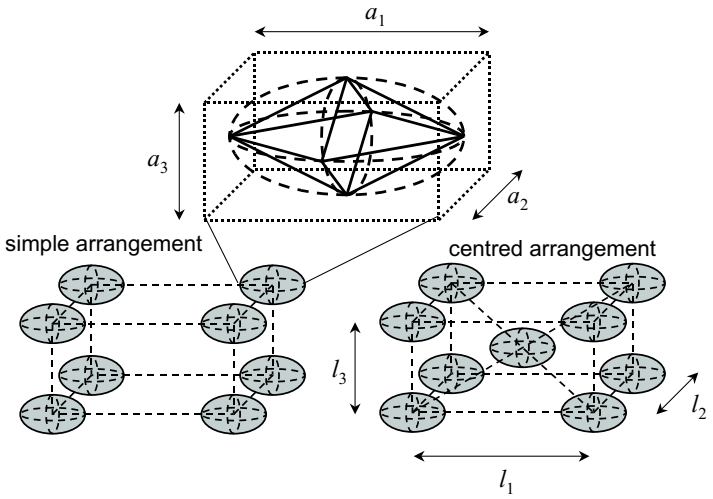

Fig. 3. Three-dimensional inclusion shapes (cuboids, ellipsoids and octahaedra) and arrangements (simple and centred) used in numerical examples

In order to minimize the numerical error and investigate the convergence of the solution, numerical tests were carried out for different mesh densities. The tests showed that for the geometries considered in this study sufficient accuracy of the solution is obtained with 40 cells in each direction – the results presented in the following sections were obtained for such numerical mesh. Further increasing of the number of cells does not significantly influence the solution (relative errors below 3%).

A typical example of the solution of the local boundary value problem for a two-dimensional case is presented in Fig. 4. The figure shows distributions of $\chi_1(y_1,y_2)$ and $\chi_2(y_1,y_2)$ functions for weakly conductive rectangular inclusions in centred arrangement ($K_2/K_1 = 10^{-4}$). The periodicity and anti-symmetry of both functions are clearly visible. Minimum and maximum values occur in the vicinity of the parts of inclusion – matrix interface which are orthogonal to the respective flow direction (y_1 or y_2).

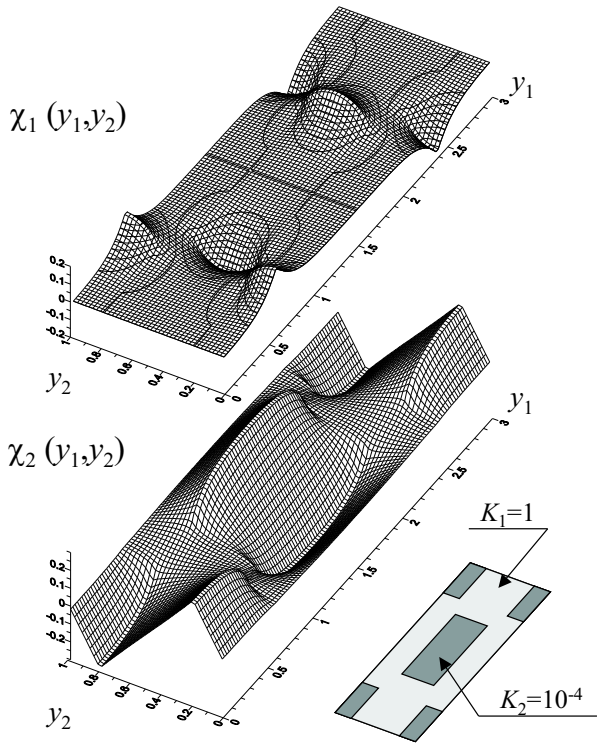

Fig. 4. Example of the distribution of χ_1 and χ_2 functions for a 2D geometry with weakly conductive inclusions

5.2. Influence of the Local Conductivity Ratio

The influence of the components' conductivity ratio on the effective conductivity of a heterogeneous soil is shown on two-dimensional examples. They concern square inclusions in simple arrangement ($f_2 = 0.49$) and rectangular inclusions in simple arrangement ($l_1 = l_2 = 1$, $a_1 = 0.9$, $a_2 = 0.5$, $f_2 = 0.45$). The relation between the effective conductivity and the inclusion conductivity K_2 is shown in Fig. 5. The values of both coefficients are calculated with respect to the matrix conductivity K_1. For rectangular inclusions both components of the effective conductivity tensor are shown. The obtained functions have sigmoidal shape, reaching constant values for large conductivity contrast. This means that for inclusions much more or much less conductive than the matrix ($K_2/K_1 < 10^{-3}$ or $K_2/K_1 > 10^3$) the effective conductivity becomes a linear function of the matrix conductivity. The linear coefficient depends on the geometry of the medium. For smaller difference of the components' conductivities the effective conductivity depends on both K_1 and K_2. Similar results (not shown here) were obtained for three-dimensional geometries.

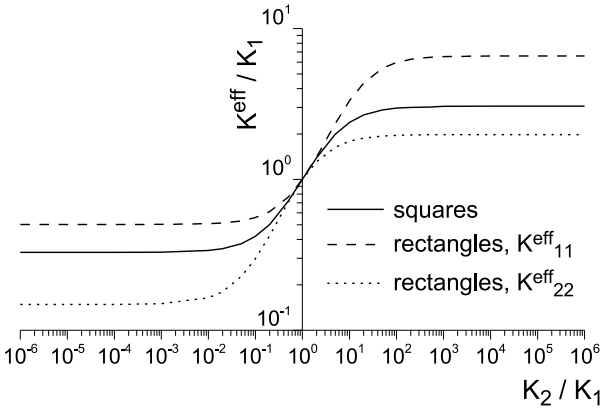

Fig. 5. Relation between the effective conductivity and the inclusion – matrix conductivity ratio K_2/K_1 for 2D inclusions

In partially saturated conditions the conductivities of both materials and their ratio are highly non-linear functions of the water pressure head h. Consequently, the effective conductivity also depends on h. This relation is shown on the example of a heterogeneous soil composed of loamy sand and silty clay. The calculations were performed for a 2D isotropic geometry with square inclusions in simple arrangement ($f_2 = 0.49$, $a_1/a_2 = l_1/l_2 = 1$, $a_1/l_1 = 0.7$). Parameters of the two materials are taken after (Carsel & Parrish 1988). The conductivity curves $K(h)$ of sand and clay cross and the parameter ratio varies in a wide range (Fig. 6). The effective conductivity function $K^{eff}(h)$ has been computed for two different cases: loamy sand matrix with silty clay inclusions and silty clay matrix with loamy sand inclusions. As one can see, the functions differ substantially from each other, since the effective conductivity strongly depends on the continuity of the most conductive material. Both effective curves have a characteristic shape – for each one two segments can be distinguished corresponding to the zones where the inclusion – matrix conductivity ratio is greater or less than one.

5.3. Influence of the Local Geometry – Isotropic Case

In this section the influence of the shape and volumetric fraction of inclusions on the effective conductivity of an isotropic medium is investigated. The calculations have been performed for 2D geometry ($a_1 = a_2$, $l_1 = l_2$) and 3D geometry ($a_1 = a_2 = a_3$, $l_1 = l_2 = l_3$). The inclusions were either much more conductive or much less conductive than the matrix ($K_2/K_1 = 10^4$ or $K_2/K_1 = 10^{-4}$). The volumetric fraction of inclusions f_2 ranged from 0 to 1, i.e. overlapping of inclusions was allowed. The limit value of f_2, for which the inclusions become connected depends on their shape and arrangement (Tabl. 1). In the two-dimensional case when the inclusions become connected the matrix loses its continuity, thus the two

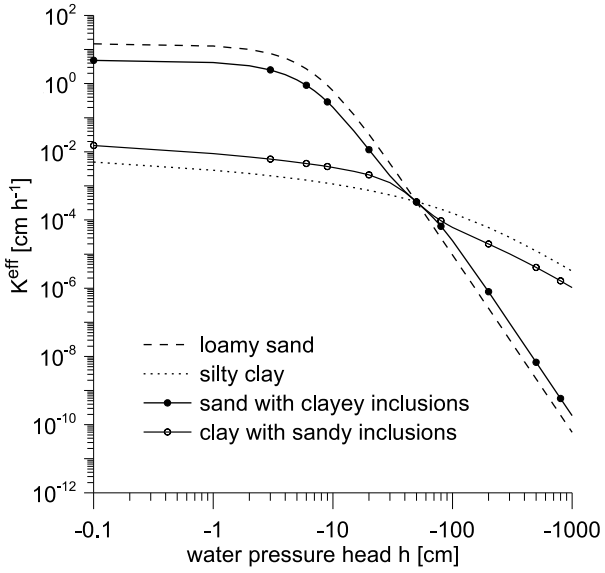

Fig. 6. Effective conductivity of an heterogeneous soil as a function of the capillary pressure head

materials interchange their roles. In the three-dimensional case the matrix keeps its continuity even for overlapping inclusions. In this case the continuity of the matrix is lost for f_2 close or equal to 1 (minimum values are 0.83 for octahedra in simple arrangement and 0.95 for ellipsoids in simple arrangement). For each analyzed case the effective conductivity calculated from the formulae (2), (4) and (6) are also shown.

Table 1. Limit value of the volumetric fraction of inclusions f_2 for which the inclusions become connected

	Arrangement	
Shape	simple	centered
rectangle	1	1/2
ellipse	$\pi/4$	$\pi/4$
rhombus	1/2	1
cuboid	1	1/4
ellipsoid	$\pi/6$	$\pi\sqrt{3}/8$
octahedron	1/6	1/3

For two-dimensional geometries (Fig. 7) K^{eff} calculated according to the homogenization theory are inside Wiener bounds (Eq. 2) and correspond to the Hashin-Shtrikman bounds (Eq. 4) – upper bound for weakly conductive inclusions and lower bound for highly conductive inclusions (note that for larger volumetric fraction f_2 inclusions and matrix interchange their roles). Bruggemann's equation

(6) gives values of K^{eff} smaller for weakly conductive inclusions and larger for highly conductive inclusions, as compared to the values obtained by homogenization. Thus, Eq. (4) seems to be a better approximation of effective conductivity for 2D periodic and isotropic geometries than Eq. (6). For small volumetric fractions of inclusions ($f_2 < 0.3$ or $f_2 > 0.8$) Eqs. (4) and (5) give very similar values of K^{eff}. The influence of shape and arrangement of inclusions on the effective conductivity seems negligible. Note the symmetry of the $K^{eff}(f_2)$ functions for $K_2 > K_1$ and $K_2 < K_1$.

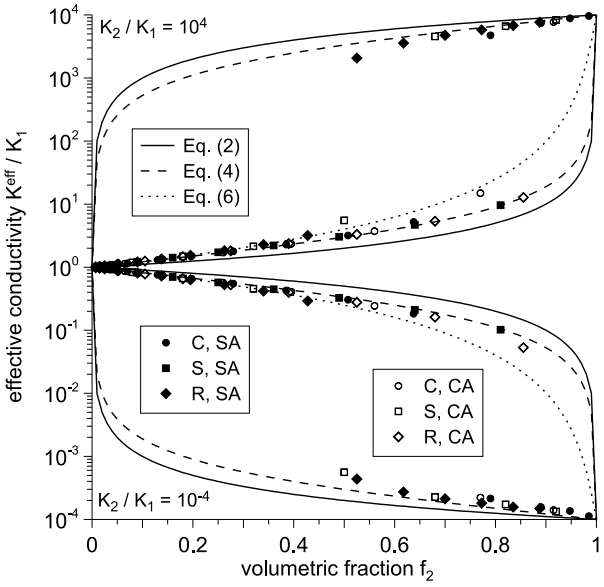

Fig. 7. Effective conductivity for 2D isotropic geometries as a function of volumetric fraction of inclusions

In the three-dimensional case (Fig. 8) a similarity of the results obtained for different shapes and arrangements of inclusions and calculated from Eq. (4) can be observed when one of the materials is discontinuous. However, there is no symmetry between the results for $K_2 > K_1$ and $K_2 < K_1$. This is due to the fact that when both materials are continuous, the effective conductivity depends on the conductivity of the most permeable material. When the highly conductive inclusions become interconnected, the effective conductivity increases rapidly by several orders of magnitude. On the other hand, when the weakly conductive inclusions become interconnected, the effective conductivity does not change significantly as long as the most permeable material keeps its continuity. However, in such situation the values of K^{eff} are somewhat smaller compared to the values obtained from Eq. (4). In this case Eq. (6) appears a better approximation, although the influence of the shape and arrangement of inclusions is more visible.

All values calculated according to the homogenization theory are inside Wiener and Hashin-Shtrikman bounds. One can also notice, that for the same volumetric fraction f_2 the effective conductivity is greater for three-dimensional geometry, than the two-dimensional one.

5.4. Influence of the Local Geometry – Anisotropic Case

A similar series of calculations has been performed for anisotropic geometries, assuming $a_1/a_2 = l_1/l_2 = 5$ for the 2D case and $a_1/a_3 = l_1/l_3 = 5, a_2/a_3 = l_2/l_3 = 2$ for 3D case. The depolarising factors are $p_1 = 0.167$, $p_2 = 0.833$ for 2D geometry and $p_1 = 0.090$, $p_2 = 0.310$, $p_3 = 0.600$ for 3D geometry. The effective conductivity is given by a diagonal tensor. The results for two-dimensional case are presented in Figs. 9 and 10. The figures show the effective conductivity in the direction of the longer and shorter axis of the inclusions, respectively. The values of K_{11}^{eff} for $K_2 > K_1$ and the values of K_{22}^{eff} for $K_2 < K_1$ obtained from homogenization are strongly dependent on the shape and arrangement of inclusions. The difference between Eqs. (4) and (6) is also significant in those cases. In other cases the analytical and numerical approximations are very close. Thus, the effective conductivity seems to be strongly related to the geometrical parameters if the flow is parallel to the longest axis of highly conductive inclusions or parallel to the shortest axis of the weakly conductive inclusions. In both cases the transport properties of the composed medium are determined by the distance between the inclusions, measured along the longest axis. In the case of highly conductive inclusions it represents the minimum thickness of the weakly permeable layer which slows down the flow, while for weakly conductive inclusions it represents the maximum size of highly conductive "gaps", which enable faster flow. One can notice some regularity of the results for different geometries. K_{ii}^{eff} is closer to the matrix conductivity for simple arrangement compared to the centred arrangement. For each of the arrangements the values closest to the matrix conductivity correspond to rectangular inclusions, while the values closest to the inclusions conductivity correspond to rhombic inclusions. At the same volumetric fraction f_2 rhombi have the largest dimensions, while rectangles have the smallest dimensions. Similar to the isotropic 2D geometries a symmetry between results for $K_2 > K_1$ and $K_2 < K_1$ is observed for anisotropic 2D geometries.

The results for three-dimensional geometries are presented in Figs. 11 and 12, showing the effective conductivity in y_1 and y_3 directions, respectively. One can observe similar differences between different shapes and arrangements of inclusions as for the two-dimensional case. However, the results for $K_2 > K_1$ and $K_2 < K_1$ do not show symmetry, due to the continuity of the highly conductive material (as in the 3D isotropic case).

Although the relations between $\mathbf{K}_{ii}^{eff}$ and f_2 described by the analytical formulae (4) and (6) roughly correspond to the numerical results obtained for periodic

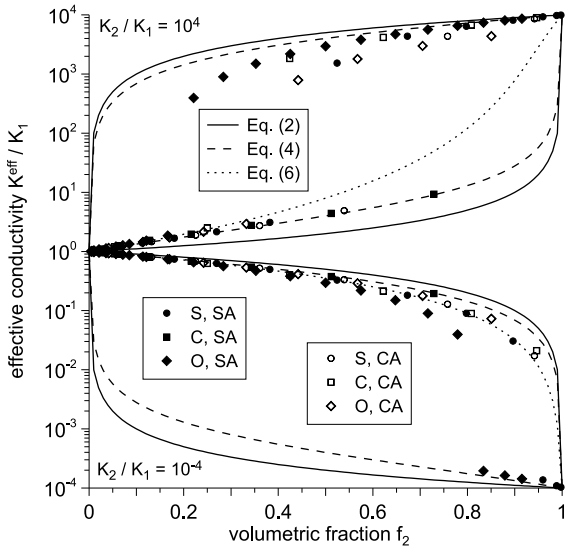

Fig. 8. Effective conductivity for 3D isotropic geometries as a function of volumetric fraction of inclusions

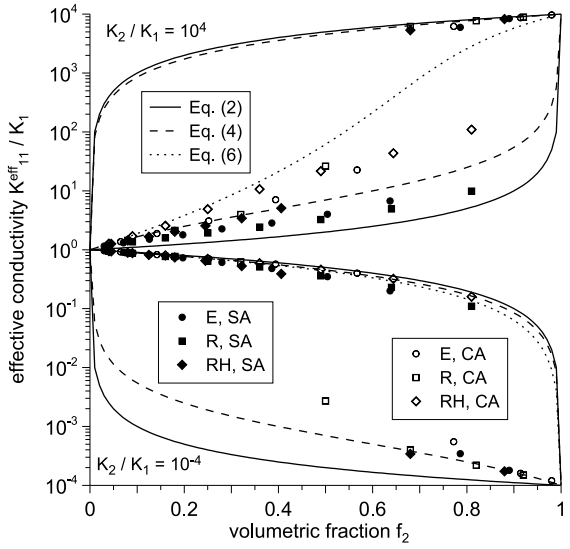

Fig. 9. Effective conductivity in y_1 direction for 2D anisotropic geometries as a function of the volumetric fraction of inclusions

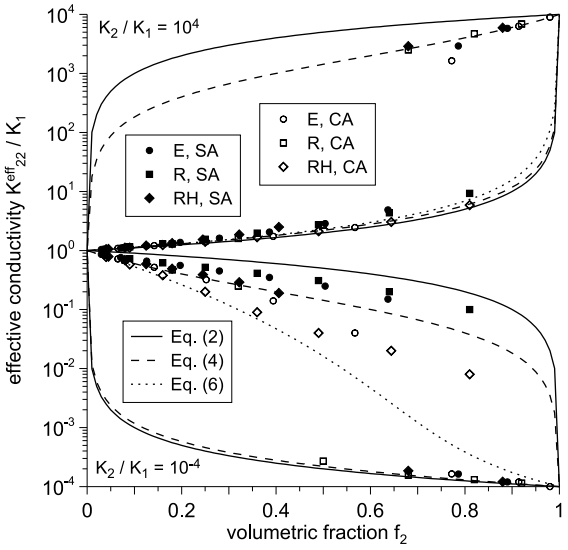

Fig. 10. Effective conductivity in y_2 direction for 2D anisotropic geometries as a function of the volumetric fraction of inclusions

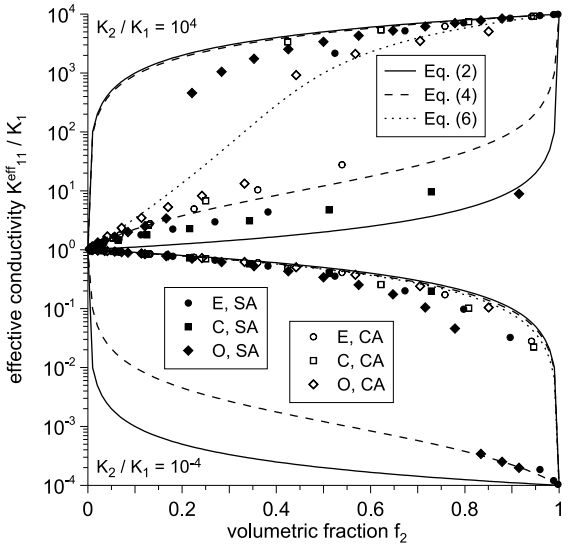

Fig. 11. Effective conductivity in y_1 direction for 3D anisotropic geometries as a function of the volumetric fraction of inclusions

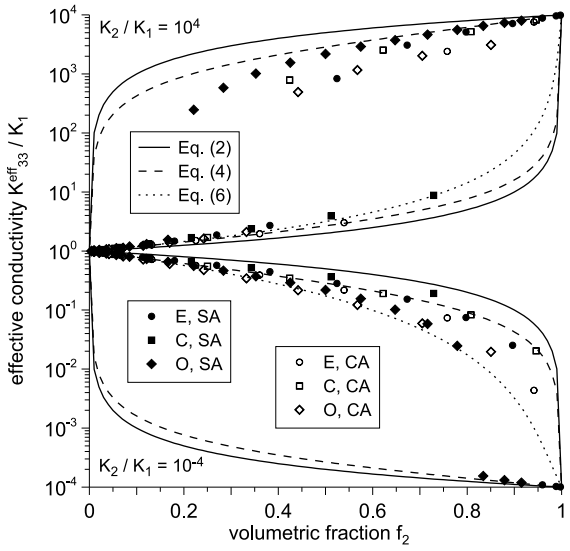

Fig. 12. Effective conductivity in y_3 direction for 3D anisotropic geometries as a function of the volumetric fraction of inclusions

geometries, they do not fit exactly to any particular geometry in the anisotropic case. In contrast to the isotropic case some values calculated numerically according to the homogenization theory fall outside the range defined by Eq. (4), however they always satisfy Wiener bounds given by Eq. (2).

6. Summary and Conclusions

Although the presented analysis is far from being exhaustive, it allows us to draw some conclusions on the effective conductivity of heterogeneous soils with periodically arranged inclusions:

- When the inclusions are much more permeable or much less permeable than the matrix, the effective conductivity becomes a linear function of the matrix conductivity, independent of the conductivity of the inclusions.
- For macroscopically isotropic media with disconnected inclusions the effective conductivity obtained for periodic geometries is very close to the effective medium approximation (i.e. Hashin-Shtrikman bounds), regardless of the shape and arrangement of the inclusions. It means that periodic and random media are equivalent in this case.
- In the case of anisotropic media the results obtained for periodic geometries show significant influence of the shape and arrangement of inclusions on the effective conductivity in some directions. None of the considered periodic geometries corresponds exactly to the effective medium approximations, although some qualitative similarity can be observed. Discrepancy of

the results for periodic and random media is also reported by other authors (e.g. Harter & Knudby 2004, Fokker 2001).

Finally, one should note that the presented approach to calculate the effective conductivity based on the homogenization theory is not limited to the simple periodic geometries considered in this paper. The method also allows investigation of more complex cases, e.g. random distribution of conductivity or local anisotropy of the components.

References

Auriault J.-L. (1991), Heterogeneous Medium: is an Equivalent Macroscopic Description Possible? *International Journal of Engineering Science*, Vol. 29, 785–795.

Bear J. (1972), *Dynamics of Fluids in Porous Media*, Elsevier.

Bensoussan A., Lions J. L., Papanicolaou G. (1978), *Asymptotic Analysis for Periodic Structures*, North-Holland.

Berryman J. G. (1995), *Mixture Theories for Rock Properties*, in: T. J. Ahrens (ed.) *American Geophysical Union Handbook of physical constants*, 205–228.

Björck A. & Dahlquist G. (1974), *Numerical Methods*, Prentice Hall.

Carsel R. & Parrish R. (1988), Developing of Joint Probability Distributions of Soil Water Retention Characteristics, *Water Resources Research*, Vol. 24, 755–769.

Crumpton P. I., Shaw G. J., Ware A. F. (1995), Discretization and Multigrid Solution of Elliptic Equations with Mixed Derivative Terms and Strongly Discontinuous Coefficients, *Journal of Computational Physics*, Vol. 116, 343–358.

Dagan G. (1989), *Flow and Transport in Porous Formations*, Springer-Verlag, New York.

Giordano S. (2003), Effective Medium Theory for Dispersions of Dielectric Ellipsoids, *Journal of Electrostatics*, Vol. 58, 59–76.

Fokker P. A. (2001), General Anisotropic Medium Theory for the Effective Permeability of Heterogeneous Reservoirs, *Transport in Porous Media*, Vol. 44, 205–218.

Harter T. & Knudby C. (2004), Effective Conductivity of Periodic Media with Cuboid Inclusions, *Advances in Water Resources*, Vol. 27, 1017–1032.

Hashin Z. & Shtrikman S. (1962), A Variational Approach to the Theory of Effective Magnetic Permeability of Multiphase Materials, *Journal of Applied Physics*, Vol. 33, 3125–3131.

Jones S. B. & Friedman S. P. (2000), Particle Shape Effects on the Effective Permittivity of Anisotropic and Isotropic Media Consisting of Aligned or Randomly Oriented Ellipsoidal Particles, *Water Resources Research,* Vol. 36, 2821–2833.

King P. (1989) The use of Renormalization for Calculating Effective Permeability, *Transport in Porous Media*, Vol. 4, 37–58.

Lewandowska J. & Auriault J.-L. (2004), Modeling of Unsaturated Water Flow in Soils with Highly Permeable Inclusions, *Comptes Rendus Mecanique,* Vol. 332, 91–96.

Lewandowska J. & Laurent J.-P. (2001), Homogenization Modeling and Parametric Study of Moisture Transfer in an Unsaturated Porous Medium, *Transport in Porous Media*, Vol. 45, 321–345.

Lewandowska J., Szymkiewicz A., Burzyński K., Vauclin M. (2004), Modeling of Unsaturated Water Flow in Double-Porosity Soils by the Homogenization Approach, *Advances in Water Resources*, Vol. 27, 283–296.

Lewandowska J., Szymkiewicz A., Gorczewska W., Vauclin M. (2005), Infiltration in a Double-Porosity Medium: Experiments and Comparison with a Theoretical Model, *Water Resources Research*, Vol. 41, W02022, doi:10.1029/2004WR003504.

Markov K. Z. (1999), *Elementary Micromechanics of Heterogeneous Media*, in: Markov K. Z. & Preziosi L. *Heterogeneous Media: Modeling and Simulation,* Birkhauser, Boston.

Poley A. D. (1988), Effective Permeability and Dispersion in Locally Heterogeneous Aquifers, *Water Resources Research*, Vol. 24, 1921–1926.

Quintard M. & Whitaker S. (1988), Two-Phase Flow in Heterogeneous Porous Media: The Method of Large-Scale Averaging, *Transport in Porous Media*, Vol. 3, 357–413.

Renard P. & de Marsily G. (1997), Calculating Equivalent Permeability: a Review, *Advances in Water Resources*, Vol. 20, 253–278.

Saez A., Otero C., Rusinek I. (1989), The Effective Homogeneous Behavior of Heterogeneous Porous Medium, *Transport in Porous Media,* Vol. 4, 213–288.

Sanchez-Palencia E. (1980), *Non-Homogeneous Media and Vibration Theory*, Springer-Verlag. Berlin.

Szymkiewicz A. (2004), *Modeling of Unsaturated Water Flow in Highly Heterogeneous Soils,* PhD dissertation, Université Joseph Fourier, Grenoble / Politechnika Gdańska, Gdańsk.

Wen X.-H. & Gómez-Hernández J.-J. (1996), Upscaling Hydraulic Conductivities in Heterogeneous Media: An overview, *Journal of Hydrology,* Vol. 183 (1–2), ix–xxxii.

Zaradny H. (1993), *Groundwater Flow in Saturated and Unsaturated Soils,* Balkema, Rotterdam/Brookfield.